Probing femtosecond plasmon dynamics with nanometer resolution

Jörg Lange, Daniela Bayer, Martin Rohmer, Carsten Wiemann, Oksana Gaier, Martin Aeschlimann, Michael Bauer*
Fachbereich Physik, University of Kaiserslautern, Erwin-Schrödinger Str. 46, 67663 Kaiserslautern, Germany

ABSTRACT

In combining time-resolved two-photon photoemission (TR-2PPE) and photoemission electron microscopy (PEEM) the ultrafast dynamics of collective electron excitations in silver nanoparticles (localized surface plasmons – LSP) is probed at femtosecond and nanometer resolution. In two examples we illustrate that a phase-resolved (interferometric) sampling of the LSP-dynamics enables detailed insight into dephasing and propagation processes associated with these excitations. For two close-lying silver nano-dots (diameter 200 nm) we are able to distinguish small particle to particle variations in the plasmon eigenfrequency, which typically give rise to inhomogeneous line-broadening of the plasmon resonance in lateral integrating frequency domain measurements. The observed spatio-temporal modulations in the photoemission yield from a single nanoparticle can be interpreted as local variation in the electric near-field and result from the phase propagation of the plasmon through the particle. Furthermore, we show that the control of the phase between the used femtosecond pump and probe laser pulses used for these experiments can be utilized for an external manipulation of the nanoscale electric near-field distribution at these particles.

Keywords: plasmon, silver-nanoparticle, femtosecond dynamics, PEEM

1. INTRODUCTION

The physics of localized collective electronic excitations in metallic nanostructures (often referred to as localized surface plasmons (LSP) or Mie-plasmons) has attracted considerable attention over decades. The complex electromagnetic fields induced at the surface particularly at excitation in or close to the resonance of these LSP are thought to be responsible for the enhancement of non-linear effects such as surface enhanced raman scattering (SERS), surface second harmonic generation, and multi-photon photoemission. The most recent interest in this field has been stimulated additionally by the potential of surface plasmons to concentrate and channel light inside subwavelength structures to be used in nanoscopic photonic circuits.[1, 2] An unambiguous experimental access to the physics of LSP resonances, particularly with respect to nanoscale shape and size effects, typically requires well-defined and monodisperse nanostructured samples which are then addressed using lateral integrating techniques.[3-7] Alternatively, microscopy techniques directly or indirectly sensitive to LSP may be applied to locally map the plasmon properties with the advantage that also heterogeneous particle distributions can be addressed reasonably.[8, 9]

Photoemission electron microscopy (PEEM) in combination with nonlinear photoemission, particularly two photon photoemission (2PPE), has just recently attracted considerable attention due to its high sensitivity to local LSP excitations combined with a lateral resolution in the sub-100 nm regime.[10-13] As the photoemission yield is governed by the local electric field distribution it can be considered as a direct probe of the LSP induced field enhancement. A highly promising further aspect is the potential of two-photon photoemission electron microscopy (2PPEEM) to be performed in a time-resolved stroboscopic mode enabling real-time experiments at a temporal resolution in the sub 100 fs-regime.[14] This allows to directly monitor the spatio-temporal dynamics of the local field distribution associated with the decay of the LSP mode. Even more, in a phase-resolved 2PPE mode accurate information on the relative phase of the LSP-mode to an oscillating reference field such as the driving external light field can be achieved.[15] In this means it may be possible to obtain a complete picture of the near-field dynamics associated with plasmon excitations in low-dimensional nanostructures.

* mkbauer@physik.uni-kl.de; phone 49 (0)631 205 2385; fax 49 (0)631 205 3903

In this paper we present two different experimental examples exemplifying the potential of phase- and time-resolved two-photon photoemission electron microscopy (PRPEEM) in probing the plasmon dynamics in nanostructured materials. The observation of the phase loss between the LSP excitations of two close lying particles proofs the exceptional local and temporal sensitivity of this technique to small differences in the LSP response. In mapping the spatio-temporal evolution of the 2PPE-yield within a single particle we are furthermore able to follow the phase-propagation of a LSP through a particle on a sub-femtosecond time-scale. This latter example illustrates furthermore how the phase-control of a laser field enables the manipulation of the local field-distribution in nanoscopic systems.

2. EXPERIMENTAL

A schematic view of the experimental setup is shown in Figure 1. The commercial PEEM instrument used for our experiments (Focus IS-PEEM) is described in detail in reference [16]. The microscope is mounted in a μ-metal chamber to shield external stray magnetic fields that would affect the imaging quality of the system with respect to the lateral resolution. The resolution that can be achieved with the microscope has been specified to < 40 nm. Two different light sources have been used to record PEEM images: a conventional mercury vapour UV source (high energy cut-off at 4.9 eV) and the frequency doubled output of a femtosecond Ti:Sapphire laser system (800 nm, 80 MHz repetition rate, 30 fs pulsewidth (FWHM)). Using the mercury vapor lamp, the lateral distribution of the near-threshold photoemission is imaged by the PEEM. At typical work functions of the investigated silver nanostructures of about 4.5 eV the photon energy of the pulsed laser source (hν=3.1 eV) is not sufficient for conventional photoemission. The high peak intensities of the femtosecond pulses give, however, rise to high two-photon photoemission (2PPE) yields so that we observe emission currents that are comparable to or even higher than those achieved in threshold photoemission with the mercury lamp. The phase- and time-resolved experiments are realized in a pump-probe configuration using a Mach-Zehnder type interferometer. Here, the second harmonic light is split into two pulses of equal intensity and polarization where a piezo-driven optical delay stage is used to temporally delay one pulse with respect to the other pulse. This setup guarantees an accuracy in the relative positioning of both interferometer arms of 20 nm corresponding to a temporal delay between the respective laser pulses traveling through the different arms of 67 attoseconds. This allows to sample the local field distribution at the surface induced by the 400 nm light (oscillation period: 1.3 femtoseconds) with interferometric temporal resolution. The performance of the interferometer has been checked by lateral integrating phase- and time-resolved 2PPE measurements from a polycrystalline tantalum sheet (see Fig. 2). The displayed data were recorded using an electron energy analyzer at a electron kinetic energy of about 6 eV (sample bias: -4 V with respect to analyzer entrance) close to the high energy cutoff of the 2PPE spectrum. The oscillation fringes due to the interference between pump- and probe pulse are clearly resolved and the accurate periodicity reproduced for these measurements over the entire temporal delay proofs the position stability of this setup.

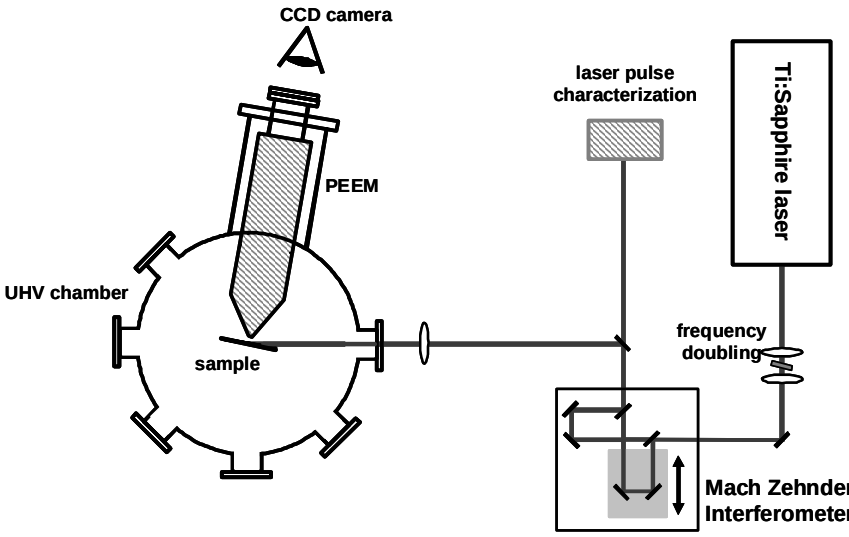

Fig. 1: The experimental setup consists of a femtosecond Ti:Sapphire laser system including a high-resolution Mach-Zehnder interferometer for phase- and time-resolved experiments and a UHV-chamber equipped with a photoemission electron microscope.

Small silver particles deposited on a 30 nm thick ITO substrate on top of a 1 mm thick glass disk were prepared using electron beam lithography as described in reference [17]. This procedure allows a controlled design of periodic arrays of nanoparticles at varying shape and distances down to the sub-50 nm regime. For the present study two different periodic arrays (size: 150 µm * 150 µm) consisting of silver nanoparticles (height: 50 nm, diameter: 200 nm) have been prepared. SEM images of sample 1 (particle pairs) and sample 2 (single particles) are shown in Figure 3. The periodicity of both arrangements is 750 nm. The centre to centre distance within the particle pairs of sample 1 is 350 nm. The LSP resonance of silver nanoparticles is in general located in the optical regime and depends in detail on the size and the shape of the particle and the dielectric response of the surrounding of the particle.[18] Two different dipolar LSP modes can be distinguished for the used single particle geometry corresponding to an excitation perpendicular and parallel to the surface, respectively. Calculations taking into account retardation effects as well as the cylindrical geometry of the particles predict the resonance energies of the LSP modes to 3.1 eV (perpendicular mode) and 2.1 eV (parallel mode), respectively. Extinction spectroscopy of the particle arrays performed at normal incidence enable to experimentally determine the resonance energy of the parallel mode to 2.1 eV in very good agreement with these predictions. Our calculations are therefore also a reliable estimate of the resonance energy of the perpendicular plasmon mode. We conclude that for p-polarized excitation[19] with the 400 nm laser light a resonant or near-resonant coupling to this perpendicular mode is accomplished. For sample 1 the close vicinity of the particles within the pairs gives rise to dipole-dipole coupling between the particles resulting in a modification of the LSP-mode spectrum.[20] Depending on particle size and particle distance a splitting into a low-energy and a high-energy mode is expected corresponding to in-phase and out-of-phase oscillation of the respective single particle modes. For the present geometry our calculations predict only weak coupling accompanied by a energy splitting much smaller than the intrinsic line-width of the LSP modes.

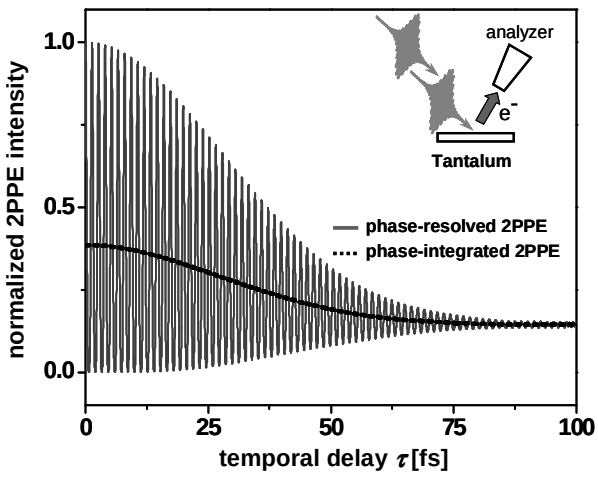

Fig. 2: time- and phase-resolved 2PPE from a polycrystalline tantalum sheet measured at an electron kinetic energy of 6.0 eV. The grey line is the measured 2PPE interferogram; the black dotted line shows for comparison data as achieved in a conventional (phase-integrated) 2PPE measurement .

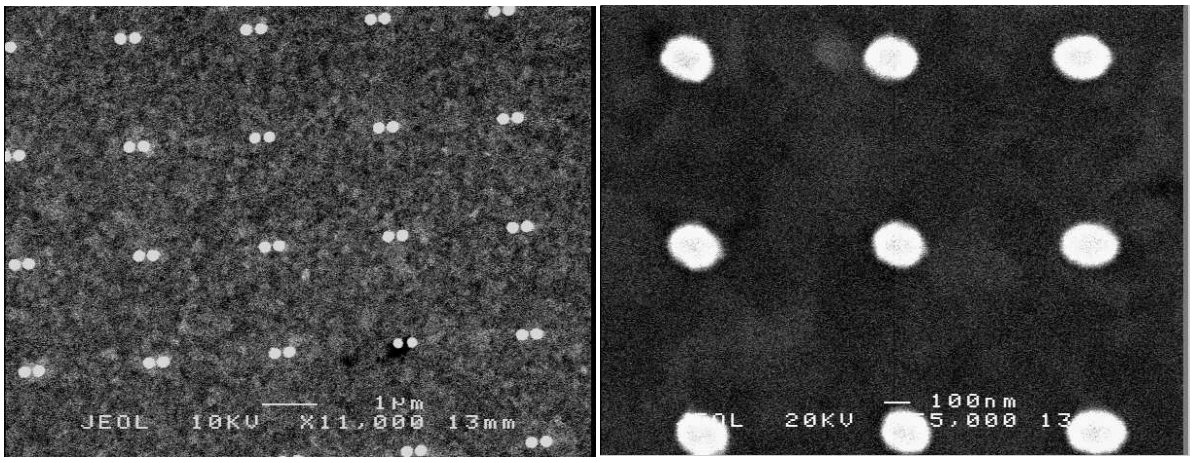

Fig. 3: SEM images of the particle pairs (sample 1, left) and the single particles (sample 2, right);

3. RESULTS AND DISCUSSION

3.1 Particle Pairs

Figure 4 shows PEEM images of sample 1 recorded in the conventional PEEM-mode (Fig. 4a) using the mercury vapour lamp (threshold photoemission) and in the 2PPEEM mode (Fig. 4b) using p-polarized 400 nm light from the femtosecond laser source. It is obvious that in both photoemission modes the lateral resolution of the PEEM enables a clear and unambiguous imaging of these sub-wavelength sized nanostructures (diameter 200 nm). Whereas the threshold image (Fig. 4a) indicates a rather homogeneous sample pretending an array of almost perfect and identical particle pairs, we observe in the 2PPE image (Fig. 4b) clear differences in the local photoemission response from the particle pairs and particles. This enhanced sensitivity of the 2PPE mode to sample inhomogeneities arises from the nonlinear (second order) dependence of the electron yield on the local field intensity of this photoemission process. In this means, slight variations in the field distribution as modified e.g. by defects undergo an effective amplification in contrast to the (linear) threshold photoemission case.

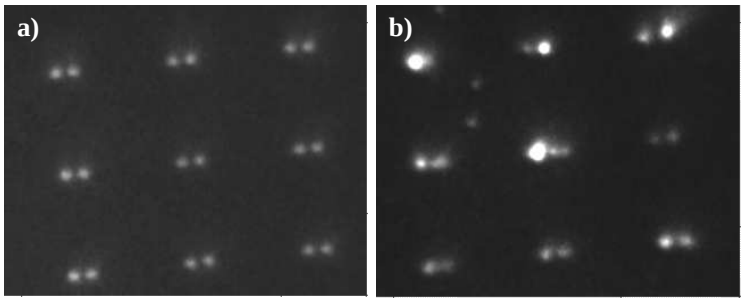

Fig. 4: PEEM images of particle pairs; a) threshold photoemission using 4.9 eV from a mercury vapour lamp; b) 2PPE image induced by 3.1 eV femtosecond laser light.

Figure 5 comprises a section from of a phase- and time-resolved 2PPEEM scan (interferogram) of a single particle (image size: 420 nm * 420 nm) and covering a time regime corresponding to two oscillation periods of the exciting 400 nm laser light. The temporal delay between two consecutive images is 0.13 fs. The visible (periodic) intensity oscillations result from the alteration between constructive and destructive interference between pump and probe laser pulse as the temporal delay (or alternatively speaking the phase delay) between both pulses is scanned. However, the mapped electron emission from the particle is in principle not governed by this external laser-field but is rather determined by the *laser-field induced* internal particle near-field related to the excitation of the LSP resonance. Therefore, next to the pump-probe interference, the temporal variation in the electron emission yield contains also information on the response of the LSP-induced near-field to the driving external laser-field. This LSP-related dynamical properties can be highlighted, for instance, in comparing these data to a reference interferogram, such as the interferogram of the pure external field (approximated, for instance, by a measurement as displayed in Fig. 2) or, alternatively, the local 2PPE interferogram of a neighbouring particle. In Figure 6 we quantitatively compare 2PPE interferograms of two neighbouring particles of sample 1 close to time-zero (perfect temporal overlap between pump and probe pulse, Fig. 6a) and at a temporal delay of about 50 fs (Fig. 6b). The interferograms were generated by displaying the lateral integrated electron emission yield from the respective particles as function of temporal delay between pump and probe pulse. Figure 6a shows that in the vicinity of the time zero of our measurement the local LSP response of both particles to the external pump-probe field is identical. Within the accuracy of our measurement we are not able to identify any deviation between both traces. However, as the temporal delay between pump and probe pulse increases, we observe a successive phase-loss in the response of the two particles so that for sufficient high temporal delays (Fig. 6b) the phase response of one particle has been significantly delayed with respect to the neighbouring

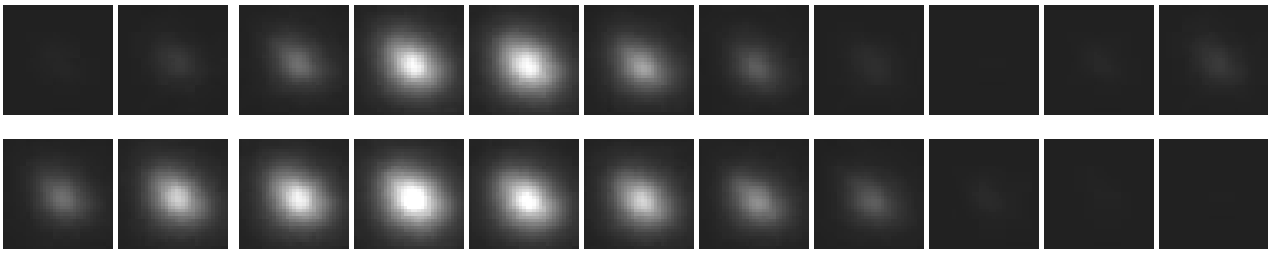

Fig. 5: section of a single particle phase-resolved PEEM scan at an excitation energy of 3.1 eV. The images are displayed at a temporal delay rate of 0.14 fs/frame.

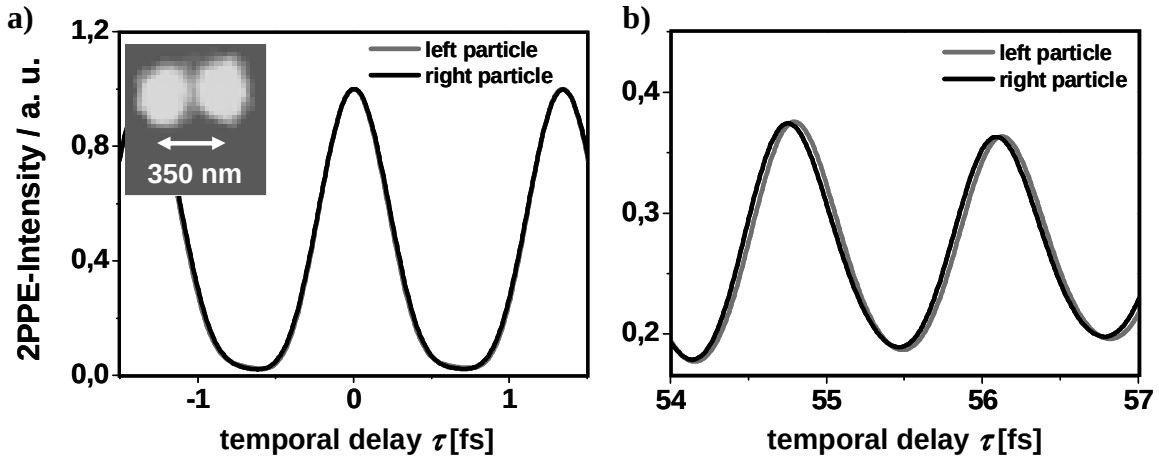

Fig. 6: comparison of sections of the 2PPE-interferograms of the two neighbouring nanoparticles of sample 1 displayed in the inset; response of the two particles to the external light field a) at time zero (temporal overlap of pump and probe pulse) and b) at large temporal delays of about 55 fs.

particle. At 55 fs this phase delay has achieved a value of about 1/40*2π. Note that even though this value seems to be rather small, it is, within the accuracy of our measurements, by far significant. A very important aspect in this means is that the imaging PEEM modus enables parallel data acquisition from both particles at the same time. For a given temporal delay between pump and probe pulse, the data displayed in Figure 6 have been recorded under absolutely identical experimental conditions so that systematic errors arising from the experimental approach are not necessary to be considered for a comparison of the local response of both particles. A similar behaviour as observed for the different response of the two neighbouring particles shown here has been reported before by Petek et. al.[15] in a PR2PPEEM study of small nanoparticles as formed by silver deposition onto mesa structures photographically formed on a quartz substrate. In agreement with our data the authors observe a divergence of the relative phase for the electron emission from different silver particles as the temporal delay increases. This behaviour is interpreted as follows: Close to time zero the field amplitude of the ultrashort laser field is dominating the local field and forces the LSP-mode (and the corresponding local near-field) to oscillate exactly at the laser frequency. As the time proceeds the laser field intensity decreases due to the limited laser pulse width. However, due to the finite lifetime of a plasmon of about 10 – 15 fs in case of silver particles[21], the LSP-mode is still oscillating for some time after the laser field has more or less disappeared. Not forced any more by an external field it is evident that at that time the LSP mode will oscillate at its particle characteristic eigenfrequency. In this view, the evolvement of a phase loss (dephasing) in the response between different particles can be assigned to differences in the eigenfrequency of the studied particles. As the plasmon eigenfrequency is governed by the size or the shape of the particles or the coupling of the particles to the underlying substrate this observation is a direct evidence for a particle to particle inhomogeneity of the sample. In case of (lateral integrating) frequency domain measurements these inhomogeneities will for instance give rise to an inhomogeneous (Gaussian) line broadening.

As mentioned above, small variations in the LSP mode eigenfrequencies in case of close lying particle pairs may also arise from the splitting into a low-energy and high-energy LSP-mode due to the dipole-dipole coupling between the particles. For the present case we exclude that this effect is a dominant contribution to the observed

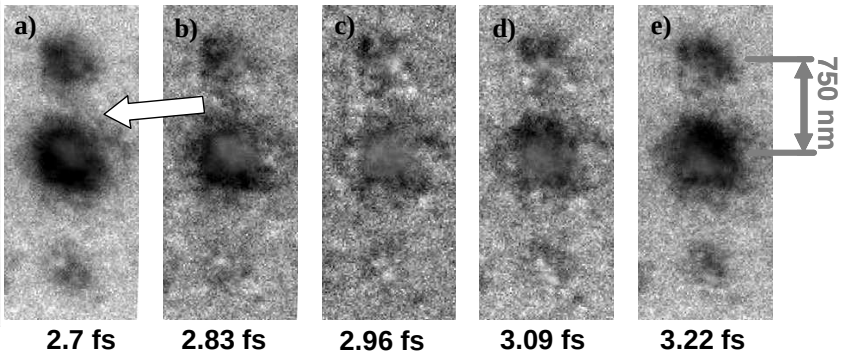

Fig. 7: Phase-resolved PEEM of three well-separated particles of sample 2 (particle diameter: 200 nm) highlighting particle-internal 2PPE-yield variations as function of the temporal delay between pump and probe laser pulse.

dephasing process. Comparison of local interferograms of different particle pairs of the sample show that the particle-particle deviations in the phase response are arbitrary, whereat the magnitude of the phase differences as well as its sign changes from particle pair to particle pair. A characteristic property intrinsic to a particle pair, e.g. as result of a dipole-dipole coupling, should give rise to a way more systematic behaviour.

3.2 Single particle sample

For the second experimental example we focused our attention to variations in the local 2PPE-yield *within* a single particle of sample 2. Figure 7 shows a series of images of three well separated particles recorded in a phase-resolved scan at time steps of 0.13 fs per image frame. Clearly visible is a modification of the local intensity distribution as function of the temporal delay between pump and probe pulse particularly for the centre particle. The image series implies that the intensity maximum of the 2PPE yield propagates from the top right to the bottom left area of the particle within a third of the oscillation period of the driving external electromagnetic field. As we associate the 2PPE intensity with the local near field at the particle surface we can assign this observation to a property of the excited LSP mode of the particle. We would like to mention that the intensity distribution shown in Figure 7 does not correspond to the actual overall 2PPE-yield distribution but that the displayed results arise from a normalization of the local 2PPE yield at the given delay by the corresponding local 2PPE yield recorded at time-zero delay. In this means any contributions to 2PPE intensity variations due to static (non-delay dependent) particle inhomogeneities related to contrast mechanism such as topography or workfunction variations are cancelled out. This procedure enables an efficient enhancement of the small, but significant variations in the delay dependent 2PPE intensity distribution.

A quantitative analysis of these PRPEEM results is displayed in Figure 8. The graph compares laterally integrated 2PPE intensities from the top right area (area B) and the bottom left area (area A) of the centre particle as function of temporal delay over two oscillation periods of the laser field (see also inset in Figure 8). Clearly visible is the phase shift in the response of area B in comparison to area A. In contrast to the particle pair example, this phase shift is not only observable at large temporal delay, but it is also clearly visible at the time-zero of the measurement. This shows that the underlying mechanism is different from that one discussed in case of the time-dependent particle pair data.

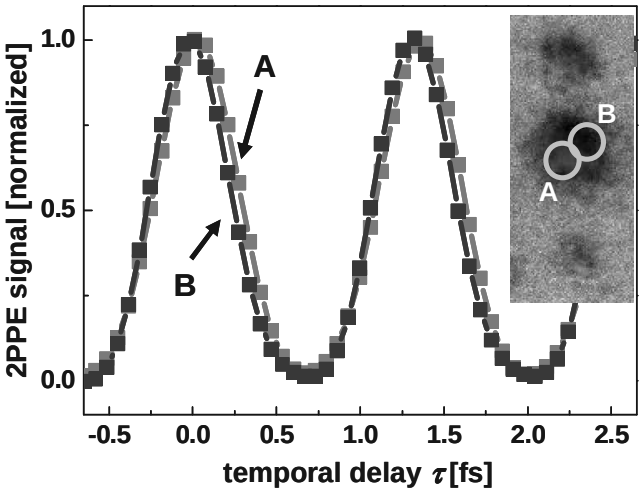

Fig. 8: Comparison of interferograms taken from different areas (A and B, see inset) of the center particle shown in Fig. 7 .

The origin of the nanoparticle internal dynamics becomes obvious, if the effect of the PEEM-intrinsic, off-normal (grazing incidence) laser illumination of the particles is considered. As we will see in the following, this artificially induced symmetry-break in the light-particle interaction is a prerequisite for the observation of a modulation in the lateral single-particle 2PPE-yield distribution. For the example displayed in Figure 7, the white arrow indicates the direction of incidence of the laser pulses projected onto the substrate plane. Consider the laser-light as plane wave incident from the right onto a particle where the electric field amplitude is determined by the phase delay $\Delta\varphi(\tau)$ between pump and probe pulse as adjusted by the Mach-Zehnder interferometer. For the following it is not necessary to consider the pulsed structure of the laser light so that the relevant temporal dependence of the total incident oscillating electric field $E_{tot}(t)$ can be written as:

$$E_{tot}(t) = E_1 \cdot e^{i\omega t} + E_2 \cdot e^{i\omega t + \Delta\varphi(\tau)} \qquad (1)$$

E_1 and E_2 are the amplitudes of the pump and probe laser field, ω is the oscillation frequency corresponding to the used photon energy of $h\nu$=3.1 eV. Incident from the right we expect the laser light to couple at first to the LSP-mode at

the right edge *(r=0)* of the particle. In a one-dimensional view this will induce at this point a locally oscillating field $E_{LSP}(t, r=0)$ of the form:

$$E_{LSP}(t, r=0) = A(\omega)e^{i\delta(\omega)} \cdot E_{tot}(t) = Ae^{i\delta(\omega)} \cdot \left(E_1 \cdot e^{i\omega t} + E_2 \cdot e^{i\omega t + \Delta\varphi(\tau)}\right) \qquad (2)$$

$A(\omega)$ can be considered as the field enhancement factor of the external field due to the coupling to the LSP mode. The phase $\delta(\omega)$ is the (frequency dependent) phase shift of the LSP response to the external field. $E_{LSP}(t, r=0)$ is the field that governs the measured 2PPE-yield from the right part of the particle mapped by the PEEM. The periodic variation in the local 2PPE intensity as function of time directly reflects the change between constructive and destructive interference of the pump and probe laser beam as the phase delay $\Delta\varphi$ (the Mach-Zehnder interferometer, respectively) is scanned.

The phase of both fields, $E_{tot}(t)$ and $E_{LSP}(t, r=0)$, will propagate along the particle, however, at different phase velocities. The external light field $E_{tot}(t)$ will give rise to a locally varying particle field $E'_{LSP}(t, r)$ of the form:

$$E'_{LSP}(t, r) = A'(\omega, r)e^{i(\delta(\omega)+\rho(r))} \cdot E_{tot}(t) \qquad (3)$$

r denotes the location at the particle and $\rho(r) = \omega/c \cdot r$ is the phase difference with respect to the 'right edge' LSP-field $E_{LSP}(t, r=0)$ governed by the phase velocity *c* of the vacuum plane wave. In a similar manner, the field induced at the particle position r by the propagating LSP-mode can be written as

$$E_{LSP}(t, r) = A(\omega, r)e^{i(\delta(\omega)+\rho_{LSP}(r))} \cdot E_{tot}(t) \qquad (4)$$

where $\rho_{LSP}(r) = \omega/v_{LSP} \cdot r$ is the propagation induced phase delay of $E_{LSP}(t, r)$ with respect to $E_{LSP}(t, r=0)$, this time governed by the phase velocity v_{LSP} of the plasmon mode in the particle. The total 2PPE yield at a given position r is obviously determined by the interference between the fields $E'_{LSP}(t, r)$ and $E_{LSP}(t, r)$. For a given pump-probe delay τ the detailed interference depends on the local phase difference $\rho(r)$- $\rho_{LSP}(r)$ so that we expect in general the overall local field amplitude $E'_{LSP}(t, r) + E_{LSP}(t, r)$ to vary with position *r*. Only for $\rho(r)=\rho_{LSP}(r)$ the phase difference between $E'_{LSP}(t, r)$ and $E_{LSP}(t, r)$ and consequently the total local field would stay constant over the entire particle. In general, we expect the phase velocity v_{LSP} of the collective excitation to be different from the vacuum phase velocity *c* of light giving rise to a phase loss between the two fields and resulting in the local 2PPE intensity modulations as observed in the experiment (Fig. 7). In this means, the particle internal structure visible in a single PEEM image of Figure 7 is a residual of the interference between external light field and the particle characteristic LSP-field. As $\rho(r)$ is exclusively governed by the well-known vacuum properties of the incidence laser light we can in principle deduce the magnitude of the LSP phase velocity v_{LSP} from these intensity modulations. For an accurate estimate, however, a phase shift between external light wave and LSP-mode of at least π along the particle extension is required. This is obviously not the case for the short 200 nm particles in this study, but requires larger (preferably elongated) particles.

So far, we considered exclusively the case of a fixed phase delay $\Delta\varphi$ (fixed temporal delay τ) between pump and probe pulse. The variation of the temporal delay τ between the two light pulses in our phase-resolved 2PPE experiments offers a further (external) degree of freedom with respect to the phase properties and therefore the local interference conditions of the entire electric field at the nanoparticle. As we can see from a comparison of different images recorded at varying τ this additional phase contribution enables an efficient manipulation of the particle internal local electric field distribution. Comparison of Figure 7a and Figure 7e shows, for example, that the maximum field amplitude can be shifted from one side of the particle to the other. We, therefore, consider the adjustment of the relative phase between pump and probe pulse by the Mach-Zehnder interferometer as an efficient means of a coherent

manipulation of the local electric field distribution in nanoscale structures. In another PEEM experiment an efficient approach for a controlled manipulation of the local field distribution (field enhancement) has just recently been demonstrated by means of a defined structuring of nanoscale particles.[11] The use of coherent light pulses for a nanoscale control of local fields has been predicted theoretically in several publications.[22] The presented results are a sucessful experimental proof of this approach. We propose that the combination of both attempts, structuring and coherent control of the exciting light, may in the future enable an extremely high flexibility in the nanoscale manipulation of local electric fields. The photoemission electron microscopy may in this context play a key role in identifying these effects.

4. CONCLUSIONS

Femtosecond time-resolved photoemission electron microscopy is a rapidly evolving experimental technique with a high potential to become one of the leading techniques in the real-time imaging of ultrafast processes at nano-structured surfaces. The two experimental examples presented in this paper highlight the capability of time- and phase-resolved 2PPEEM to map femtosecond dynamics associated with plasmon excitations at sub-wavelength resolution. The parallel image acquisition of PEEM guarantees in this context to resolve even very small lateral variations in the local dynamical behaviour as, for instance, shown in the case of the particle pair example. The identified evidence for a phase-propagation of a plasmon mode through an extended nanoparticle is a first step towards a direct imaging of the ultrafast dynamics of energy flow through nanoscopic devices, a task of high relevance e.g. for the understanding and the optimization of nanoscopic photonic circuits. A further aspect that has been addressed in this paper is the external manipulation of the lateral near-field distribution in nanoscale structures by the phase-control of the exciting femtosecond laser field. We have shown that also in this regard PEEM is the technique of choice to visualize and proof such a control scenario. A very promising approach to perform these kinds of control experiments in the future will be the application of feedback-controlled femtosecond pulse-shaping techniques.

5. ACKNOWLEDGEMENT

The authors would like to thank the Nano-Bio Center at the University of Kaiserslautern and the group of Prof. Aussenegg (TU Graz) for their support in preparing the silver nanoparticle samples.

REFERENCES

1. A.V. Zayats and I.I. Smolyaninov, J. Opt. A: Pure Appl. Opt **5** 16 (2003).
2. W.L. Barnes, A. Dereux, and T.W. Ebbesen, Nature **424**, 824 (2003).
3. B. Lamprecht, G. Schider, R.T. Lechner, H. Ditlbacher, J.R. Krenn, A. Leitner, and F.R. Aussenegg, Phys. Rev. Lett. **84**, 4721 (2000).
4. S. Linden, J. Kuhl, K. Giessen, Phys. Rev. Lett. **86**, 4688 (2001).
5. J. Lehmann, M. Merschdorf, W. Pfeiffer, A. Thon, S. Voll, and G. Gerber, Phys. Rev. Lett. **85**, 2921 (2000).
6. H. Hövel, S. Fritz, A. Hilger, U. Kreibig, M. Vollmer, Phys. Rev. B **48**, 18178 (1993).
7. F. Stietz, J. Bosbach, T. Wenzel, T. Vartanyan, A. Goldmann, and F. Träger, Phys. Rev. Lett. **84**, 5644 (2000).
8. J.-C. Weeber, J. R. Krenn, A. Dereux, B. Lamprecht, Y. Lacroute, J. P. Goudonnet, Phys. Rev. B **64**, 045411 1 (2001).
9. C. Sönnichsen, T. Franzl, T. Wilk , G. von Plessen, J. Feldmann, O. Wilson, P. Mulvaney, Phys. Rev. Lett. **88**, 077402 (2002).
10. M. Cinchetti., D.A. Valdaitsev, A. Gloskovskii, A. Oelsner,, S.A. Nepijko, and G. Schönhense, J. Electr. Spec. Rel. Phen. **137–140**, 249 (2004).
11. M. Cinchetti, A. Gloskovskii, S. A. Nepjiko, G. Schönhense, H. Rochholz and M. Kreiter, Phys. Rev. Lett. **95**, 047601 (2005)
12. G H. Fecher, O. Schmidt, Y. Hwu, and G. Schönhense, J. Electr. Spectr. Rel. Phen. **126**, 77 (2002).
13. M. Munzinger, C. Wiemann, M. Rohmer. L. Guo, M. Aeschlimann, and M. Bauer, New J. Phys. **7**, 68 (2005).
14. O. Schmidt, M. Bauer, C. Wiemann, R. Porath, M. Scharte, O. Andreyev, G. Schönhense, and M. Aeschlimann, Appl. Phys. B **74**, 323 (2002).
15. A. Kubo, K. Ondo, H. Petek, Z. Sun, Y.S. Jung, and H.K. Kim, Nano Letters **5**, 1123 (2005).

16. W. Swiech, G.H. Fecher, Ch. Ziethen, O. Schmidt, G. Schönhense, K. Grzelakowski, C.M. Schneider, R. Frömter, H.P. Oepen, and J. Kirschner, J. Elec. Spec. Rel. Phenom. **84**, 171 (1997).
17. W. Gotschy, K. Vonmetz, A. Leitner, and F.R. Aussenegg, Appl. Phys. B **63**, 381 (1996)
18. U. Kreibig and M. Vollmer, *Optical Properties of Metal Clusters*, Springer Series in material science V. 25, Springer, Heidelberg (1995).
19. for p-polarized light the electric field vector of the incident laser pulse is oriented parallel to the plane defined by the normal of the substrate surface and the k-vector of the laser pulse.
20. W. Rechberger, A. Hohenau, A. Leitner, J.R. Krenn, B. Lamprecht, and F.R. Aussenegg, Opt. Comm. **220**, 137 (2002).
21. B. Lamprecht, A. Leitner, and F.R. Aussenegg, Appl. Phys B **68**, 419 (1999).
22. M.I. Stockman, S.V. Faleev, and D.J. Bergman, Phys. Rev. Lett. 88, 067402 (2002); T. Brixner, F.J. García de Abajo, J. Schneider, and W. Pfeiffer, Phys. Rev. Lett. 95, 093901 (2005).